J Solid State Electrochem
DOI 10.1007/s10008-017-3695-z

ORIGINAL PAPER

Polyethylene oxide-based nanocomposite polymer electrolytes for redox capacitors

K. S. Perera[1] · **K. P. Vidanapathirana**[1] · **B. Jayamaha**[2] · **L. Wewagama**[2] · **M. A. K. L. Dissanayake**[3] · **G. K. R. Senadeera**[3,4] · **K. Vignarooban**[2]

Received: 10 May 2017 / Revised: 2 July 2017 / Accepted: 3 July 2017

Abstract In this work, the use of a polyethylene oxide-based nanocomposite polymer electrolyte (NCPE) in a redox capacitor with polypyrrole electrodes has been studied. To the best of our knowledge, not much work has been reported in the literature on redox capacitors fabricated using NCPEs. The composition of the polyethylene oxide (PEO)-based NCPE was fine tuned to obtain films with the highest ionic conductivity. They were mechanically stable to handle for any purpose without damaging the film. The optimized composition was {[(10PEO:$NaClO_4$) molar ratio]: 75 wt.% propylene carbonate (PC)}: 5 wt.% TiO_2. This electrolyte film showed an ambient temperature ionic conductivity of 5.42×10^{-3} S cm^{-1}. It was employed in a redox capacitor with polypyrrole electrodes polymerized in the presence of sodium perchlorate in non-aqueous medium. Performance of the redox capacitors were observed using cycling voltammetry, electrochemical impedance spectroscopy, and galvanostatic charge discharge test. It was possible to observe a satisfactory capacitive behavior in the range 58–83 F/g. Further, the redox capacitors had the ability to retain for continuous charge discharge processes.

Keywords Nanocomposite polymer electrolytes · Redox capacitors · Cyclic voltammetry · Polyethylene oxide

Introduction

Since the launching of the studies on polymer electrolytes by Fenton et al. in 1973 and follow-up actions taken by Armand et al., research activities on this class of materials have received an ever increasing interest both in academia and industry [1, 2]. Due to the potentially promising applications such as batteries, super capacitors, sensors, and solar cells, attention on polymer electrolytes has inspired an intense research and development covering various aspects including synthesis and characterization of new polymer electrolytes and improving their properties. From the beginning, polyethylene oxide (PEO)-based polymer electrolytes have spurred an enormous amount of global research. However, due to the unending research activities, it has later been realized that a high concentration of crystalline phase exists in PEO and that impedes the ionic conductivity [3]. One strategy that has been attempted to inhibit this crystallinity is by introducing nanosize filler particles such as titanium dioxide (TiO_2), silicon dioxide (SiO_2), and alumina (Al_2O_3) to PEO-based polymer electrolytes. These electrolytes were named as nanocomposite polymer electrolytes (NCPE) [4–6]. Apart from diminishing the crystalline nature of the polymer, this nanoparticle dispersion is assumed to be creating interfaces between the polymer and the nanoparticles which act as preferential ion conduction path ways. Also, mechanical stability, electrolyte/electrode contacts, and interfacial properties are substantially improved upon introduction of nanofillers. Such PEO-based NCPEs have been extensively investigated for fabricating various types of batteries [7, 8].

Today, there is a considerable interest on super capacitors compared to several decades ago. Super capacitors are ideally suited for rapid storage and release of energy during short time pulses [9]. Basically, there are two types of super capacitors, namely redox capacitors and electric double-layer capacitors

---

✉ K. S. Perera
kumudu31966@gmail.com

[1] Department of Electronics, Wayamba University of Sri Lanka, Kuliyapitiya, Sri Lanka

[2] Department of Physics, University of Jaffna, Jaffna, Sri Lanka

[3] National Institute of Fundamental Studies, Hantana, Kandy, Sri Lanka

[4] Open University of Sri Lanka, Nawala, Nugegoda, Sri Lanka

(EDLCs). Redox capacitors use conducting polymers and transition metal oxides as electrodes whereas EDLCs use carbon-based electrodes [10]. Because of this, the charge storage mechanisms of the two types are different [11]. Conducting polymers represent an attractive class of materials having the advantages such as fast doping and dedoping during charging and discharging, high charge density, low cost, and easy synthesis. A considerable amount of research work has been done on redox capacitors using conducting polymer electrodes. However, many of these redox capacitors have been fabricated using liquid electrolytes and posses the usual drawbacks due to the presence of the liquid phase. To overcome these drawbacks, gel polymer electrolytes (GPEs) have been developed as a better alternative [12, 13].

This paper describes the performance of a redox capacitor fabricated with a PEO-based NCPE and conducting polymer electrodes. Many of the PEO-based NCPEs that have been reported were based on PEO, a salt, and a nanofiller. But, in the NCPE reported in this work, propylene carbonate (PC) has also been introduced with the aim of enhancing amorphous nature and thereby increasing the conductivity. To the best of our knowledge, a redox capacitor based on a NCPE and conducting polymer electrodes has not been reported in literature.

Experimental

Preparation of PEO-based nanocomposite polymer electrolytes

PEO (Mw ~400,000, Aldrich), sodium perchlorate ($NaClO_4$) (>99%, Aldrich), and PC (99%, Aldrich) were vacuum dried at 50 °C for 24 h prior to use. Required amounts of PEO and $NaClO_4$ were added to acetonitrile (BDH) and stirred overnight using a magnetic stirrer until a homogenous mixture was obtained. The mixture was then poured into a Teflon petri dish and the solvent was allowed to evaporate. Six different samples were prepared by varying the molar ratio of PEO/Na as 5, 10, 15, 20, 25, and 30. After determining the composition that results the highest conductivity, samples were prepared adding six different weight percentages of PC to that sample. Different weight percentages of TiO_2 (P-25 Degussa) were added to the sample with the optimized PC/PEO/$NaClO_4$ composition.

AC conductivity measurements

A circular shaped sample was cut from the electrolyte film and was sandwiched between two well cleaned stainless steel (SS) discs. This sample assembly was loaded inside a Teflon sample holder which is sealed by means of an O-ring. Impedance data were collected in the frequency range from 0.1 MHz to 0.01 Hz and in the temperature range from 25 to 65 °C using a Metrohm Autolab M101 impedance analyzer.

The conductivity of the electrolyte (σ) was calculated from the equation, $\sigma = (1/R)\,(t/A)$ where t and A are the thickness and area of the electrolyte respectively and R is the bulk electrolyte resistance.

DC polarization test

The same sample assembly used for ac conductivity measurements was used to carry out the DC polarization test. The current variation across the electrolyte sample with time was monitored under a DC voltage of 1 V. Ionic transference number, t_i, was calculated using the equation. $t_\mathrm{i} = \frac{I_\mathrm{i} - I_\mathrm{s}}{I_\mathrm{s}}$ where I_i is the initial current due to ions and electrons and I_s is the saturated current due to electrons.

Preparation of conducting polymer electrodes

Pyrrole (Aldrich, 99%) was distilled and stored in dark in a refrigerator prior to use. A 0.1-M pyrrole solution was electrochemically polymerized onto fluorine-doped tin oxide (FTO) conducting glass plates using a standard three electrode setup. A Ag/AgCl electrode and a Pt electrode were used as reference and counter electrode, respectively. A non-aqueous electrolyte containing propylene carbonate (PC) (Aldrich, 99%) and 0.05 M sodium perchlorate ($NaClO_4$) (>99%, Aldrich) was used for polymerization. The current density used was 0.25 $mAcm^{-2}$ and polypyrrole (PPy) electrode film thickness was 2 μm. The cross-section area of an electrode was 1 cm^2.

Fabrication of redox capacitors

An electrolyte sample was sandwiched in between two FTO glass plates on which pyrrole was polymerized. The area of the redox capacitor was 1 cm^2.

Characterization of redox capacitors

Cyclic voltammetry

Cycling was done at the scan rate of 20 mVs^{-1} within the potential window ranging from (−1.0 to +1.0 V) to (−2.0 to +2.0 V). Measurements were taken at room temperature.

Single electrode specific capacity, C_s was calculated using the following equation. $C_s = (2\int I\mathrm{d}v)/s\,.\,\Delta V.\,m$ Here, $I\mathrm{d}v$ is the area of the CV, s is the scan rate, ΔV is the potential window, and m is the mass of a single electrode.

Electrochemical impedance spectroscopy

Impedance measurements of the redox capacitor were taken at room temperature from 0.4 MHz to 0.005 Hz. Bode plots were drawn to observe the capacitive and resistive effects as well as to find out the relaxation time (τ). $\tau = 1/2\pi f_0$ where f_0 is the frequency corresponding to the maximum imaginary capacity that is available in the graph of C'' vs f. In addition, the single electrode specific capacitance, C_s was traced with the maximum C' value in the Bode plot between C' and f [14]. Nyquist plots drawn between imaginary and real impedances were also used to calculate the single electrode specific capacitance, C_s using the equation, $C_s = 1/2\pi f Z'' m$. Here, f is a low-frequency value where capacitive features become dominant, Z'' is the imaginary value of impedance at frequency, f and m is the mass of a single electrode.

Galvanostatic charge discharge test

Redox capacitors were charged and discharged continuously under a constant current of 10 μA. Charging and discharging were terminated at the potentials of 1.5 and 0.8 V, respectively. Measurements were taken for 1000 cycles. The single electrode discharge capacity, C_d, was calculated from $C_d = \frac{I\Delta t}{m\Delta v}$. Here, I is the discharge current, m is the mass of a single electrode, and ($\Delta v/\Delta t$) is the rate of potential drop excluding IR drop during discharging.

Results and discussion

Optimization of electrolyte composition in terms of PEO/NaClO$_4$

Figure 1 shows the variation of the conductivity of the PEO/NaClO$_4$ polymer electrolyte with PEO/NaClO$_4$ molar ratio at different temperatures. Upon increasing temperature, conductivity of the electrolyte samples has increased. This is evidently due to the increase in ionic mobility when ions gain thermal energy. And also, this may be resulting from the increased amorphous nature of the PEO in the electrolyte [15, 16]. From the figure, it is seen that conductivity maxima (1.08×10^{-4} S cm^{-1} at room temperature) occurs at PEO/NaClO$_4$ molar ratio = 10 for all the measured temperatures. At very low PEO/Na ratios, the salt concentration is too high and therefore the ion concentration is high. Due to that, ions are very close to each other and there exists a high tendency to form ion pair, triplets, and aggregates which are not supporting ionic conductivity. This results a low ionic conductivity around mole ratio of PEO/Na = 5. As the ratio PEO/Na increases, salt concentration reduces and aggregation of ions gets disturbed. As a result, mobile ions are present in the system and the conductivity increases giving the maximum ionic conductivity at PEO/Na = 10. Further increase in PEO/Na ratio results in higher viscosity of the medium disrupting the migration of ions. This eventually reduces the conductivity. When PEO/Na ratio is varied from 20 to 25, an increase of conductivity is observable. This may happen when the free mobile ion concentration dominates the viscosity of the medium. At PEO/Na ratio of 25, a secondary maxima occurs with conductivity reduction beyond that point. This may be due to overruling the free mobile ion concentration by the viscosity. And also, at high PEO/Na ratios, salt concentration is very low. Then the contribution of the salt to disturb the semicrystalline nature of the electrolyte may be small [8]. As a result, conductivity can reduce.

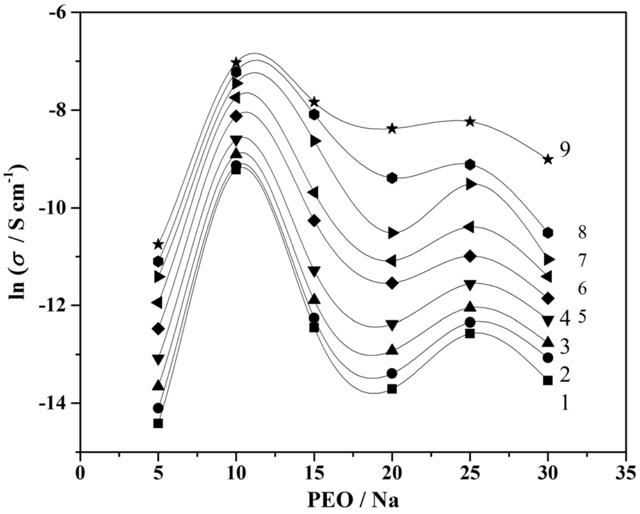

Fig. 1 Variation of the conductivity of the PEO/NaClO$_4$ polymer electrolyte with PEO/NaClO$_4$ molar ratio at different temperatures (*1*: 25 °C, *2*: 30 °C, *3*: 35 °C, *4*: 40 °C, *5*: 45 °C, *6*: 50 °C, *7*: 55 °C, *8*: 60 °C, *9*: 65 °C)

Figure 2 shows the variation of conductivity with propylene carbonate (PC) concentration of the PEO/Na = 10 electrolyte sample with the highest ionic conductivity. Upon increasing PC concentration, conductivity increases and after a maximum, it decreases. The initial conductivity increase can be attributed to the increase of the amorphous phase of the system. It is known that the glass transition temperature is lowered upon introduction of solvents such as PC and with that, crystalline phase tend to vanish. At amorphous state, polymer chains become more flexible and segmental motion increases facilitating the ionic migration. As a result, conductivity increases substantially. At higher PC concentrations, there is a possibility to form non-conducting clusters which diminish conductivity. The optimum PC concentration was taken as 75% by weight which yielded a conductivity value of 5.04×10^{-3} S cm^{-1}.

Figure 3 shows the variation of the conductivity at different temperatures for different TiO$_2$ concentrations. With increasing TiO$_2$ content, the conductivity has increased followed by a

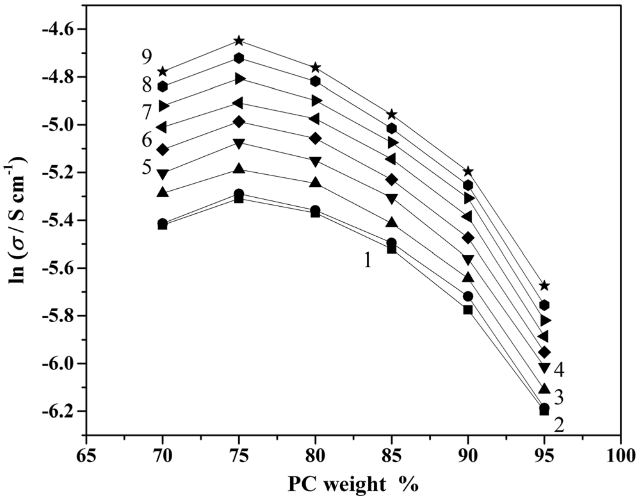

Fig. 2 Variation of the conductivity with PC concentration (by weight %) at different temperatures (*1*: 25 °C, *2*: 30 °C, *3*: 35 °C, *4*: 40 °C, *5*: 45 °C, *6*: 50 °C, *7*: 55 °C, *8*: 60 °C, *9*: 65 °C)

maximum and then decreased. Initial increase may possibly be due to the suppression of the crystalline phase by the presence of TiO_2 as well as due to the presence of additional conducting pathways formed by Lewis-acid type interactions between oxygen and OH groups at the surface of TiO_2 grains with cations in the PEO electrolyte [17, 18].

At TiO_2 concentrations higher than 5 wt%, it is very likely that these additional conduction path ways may be blocked by excess TiO_2 grains. At higher TiO_2 contents, PEO backbone may undergo gauche arrangement which restrains the segmental motion. This is not favorable for ion transport at all. Then, this leads to a substantial reduction of conductivity. The composition with 5 wt% of TiO_2 was taken as the electrolyte with maximum conductivity of 5.42×10^{-3} S cm^{-1} at 30 °C. This value is very much higher than the conductivity values reported by many groups. Nimah et al. have observed an increase of conductivity from 1.35×10^{-4} to 2.62×10^{-4} S cm^{-1} due to addition of 5% TiO_2 by [10]. Dey et al. have reported a maximum conductivity of 2.15×10^{-3} S cm^{-1} for a NCPE based on PEO, potassium iodide (KI), and cerium oxide (CeO_2) [19].

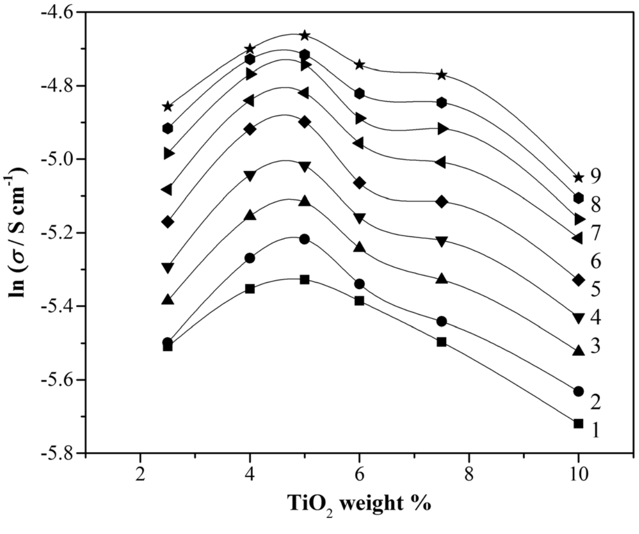

Fig. 3 Variation of the conductivity with TiO_2 concentration (by weight %) at different temperatures (*1*: 25 °C, *2*: 30 °C, *3*: 35 °C, *4*: 40 °C, *5*: 45 °C, *6*: 50 °C, *7*: 55 °C, *8*: 60 °C, *9*: 65 °C)

Ionic transference number measurements

The results of the DC polarization test with an applied voltage of 1.0 V, in the form of the variation of current with time, are shown in Fig. 4. This clearly shows that the PEO-based nanocomposite electrolyte is predominantly an ionic conductor.

It can be noticed that an initial current of 0.205 A dropped quickly to 0.01 A which is due to the ions blocked by the electrodes [20]. The calculated ionic transference number, t_i, is 0.90 confirming that the nanocomposite polymer electrolyte is predominantly an ionic conductor [21, 22].

Characterization of redox capacitors

Cyclic voltammetry

Figure 5 shows the resulting cyclic voltammograms of the redox capacitor in the configuration, PPy: ClO_4/NCPE/PPy: ClO_4. Appearance of peaks confirms the occurrence of faradaic reactions that lead to pseudo-capacitive behavior which is accompanied only by an electron charge transfer between the electrolyte and electrodes. No chemical reaction takes place under this situation. Sharp anodic and cathodic peaks are appearing in each potential window suggesting that the ion doping and dedoping occur during cycling. In addition, this is due to potential dependent capacitance. Anodic and

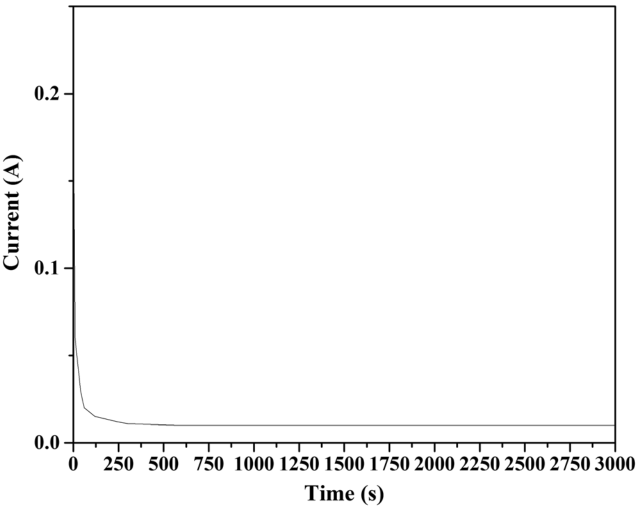

Fig. 4 DC polarization curve taken with configuration SS/NCPE/SS under 1.0 V DC voltage. *SS* stainless steel

cathodic currents increased proportionally with the potential. This is an evidence for the satisfactory reversibility of the charge discharge processes. All CV patterns exhibit a nearly mirror image symmetry of current response and this demonstrates the reversibility of the redox capacitor [23, 24].

Single electrode specific capacitance (C_s) values were calculated for each potential window and it was seen that the maximum value of C_s can be obtained within the potential window, −1.4 to +1.4 V. This observation proves that there is a dependency of C_s on the potential window which is further confirmed by the peaks in the cyclic voltammograms. At narrow potential windows, complete redox reactions of ion exchange may not take place. Also, at wider potential windows, there is a possibility for the occurrence of some other reactions such as deterioration of the conducting polymer, growth of interfacial layer between the electrolyte-electrode which hinder the proper charge storage. The highest C_s value was calculated as 83 F g^{-1}. As the polypyrrole electrodes were prepared in aqueous medium, a larger potential window, higher than 1 V was possible. If an aqueous medium was used, the potential window is restricted to 1 V as reported by Ramya et al. [25]. And also, within the potential windows considered, electrolyte seems to be stable. But, the PPy films are normally having a dense nature. This leads to limited access to the interior sites of the polymer for dopant ions lowering storage of charges.

Electrochemical impedance spectroscopy (EIS)

Figure 6a, b shows the Bode plots of the redox capacitor fabricated in the configuration, PPy: ClO_4/NCPE/PPy: ClO_4. Variation of the real part of the capacitance (C') with frequency shows that in the low-frequency region, the capacitive features become dominant where as at higher frequency region, the resistive features become dominant as reported by Tey et al. [13]. The C_s value derived from the Bode plot is 58 F g^{-1}. Relaxation time constant is 21 s. This is a very small value and it suggests the relatively fast speed of the charging discharging processes.

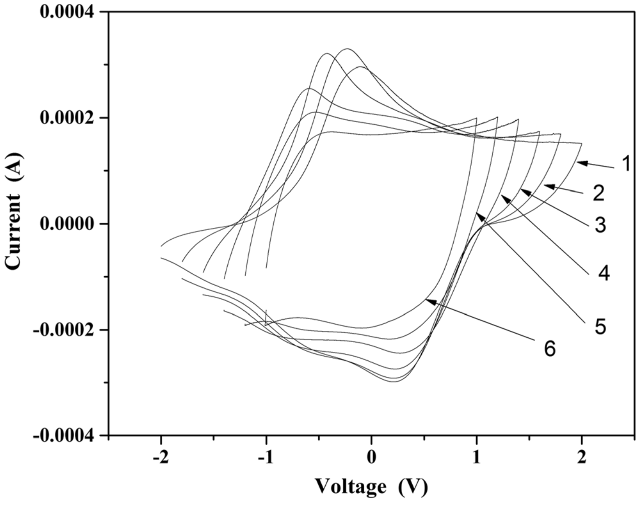

Fig. 5 Cyclic Voltammograms obtained for the redox capacitor, PPy: NCPE: PPy at different potential windows (*1*: −2 to 2 V, *2*: −1.8 to 1.8 V, *3*: −1.6 to 1.6 V, *4*: −1.4 to 1.4 V, *5*: −1.2 to 1.2 V, *6*: −1.0 to 1.0 V)

In the Nyquist plot (Fig. 7), high-frequency region is usually reflecting the properties of bulk electrolyte as a semicircle. Intermediate frequency range is exhibiting the charge transfer between electrolyte and electrodes. Another semicircle appears to represent those characteristics. At lower frequencies, resistive nature vanishes and as a result, ion migration increases. Then, impedance is determined by the ion diffusion and it gives a linear behavior. Initially, a linear portion of about a 45° angle appears in the low-frequency region of the impedance plot representing the diffusion called Warburg diffusion. As frequency is reduced further, slope of the impedance plot increases and becomes parallel to the imaginary axis exhibiting pure capacitive behavior. Absence of the high-

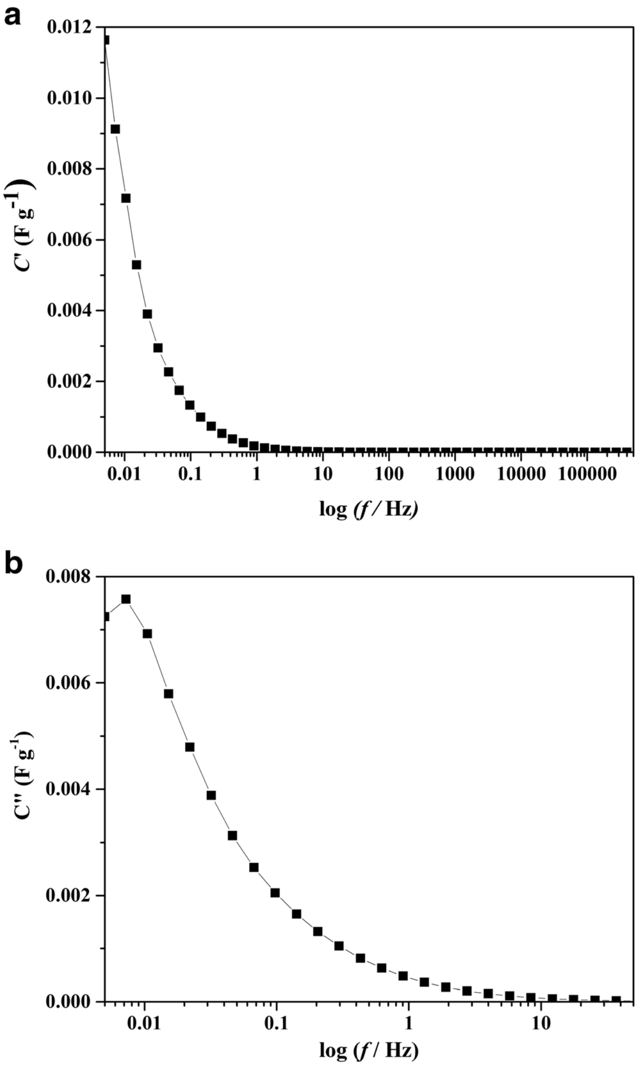

Fig. 6 **a**, **b** Bode plots drawn as real capacitance versus frequency and imaginary capacitance versus frequency, respectively

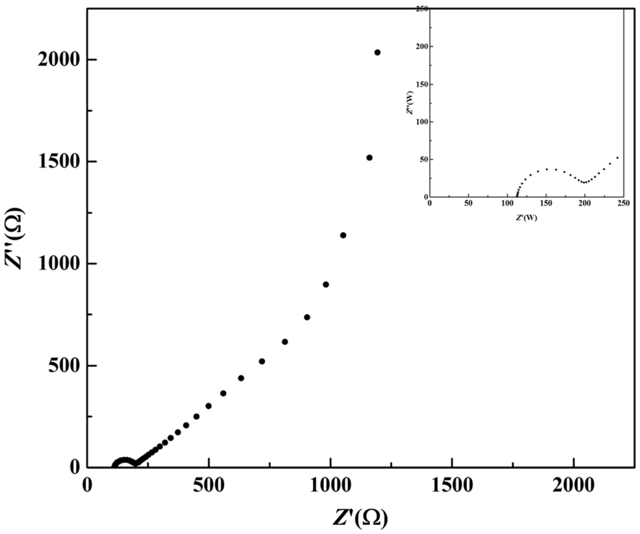

Fig. 7 Resulting Nyquist plot of the redox capacitor, PPy: NCPE: PPy (*Inset*: expanded area at high-frequency range)

frequency semicircle in the resulting impedance plot (as clear in the insert of Fig. 7) may be due to the unavailability of the required frequency range in the measurements. C_s value was calculated at the lowest frequency of 0.005 Hz and it was 65 F g^{-1}. It is very clear that the two values obtained with Bode plots and Nyquist plots are nearly same.

C_s values obtained from CV test and EIS are slightly different. It may be because in CV test, cycling is done at a constant scan rate within a potential window and for EIS, and C_s is calculated using impedance values with respect to frequency. And also, based on the selection of the frequency in the impedance plot, C_s value can vary.

Anyway, the reported values are comparatively higher than the values reported in literature for other super capacitor configurations [26, 27].

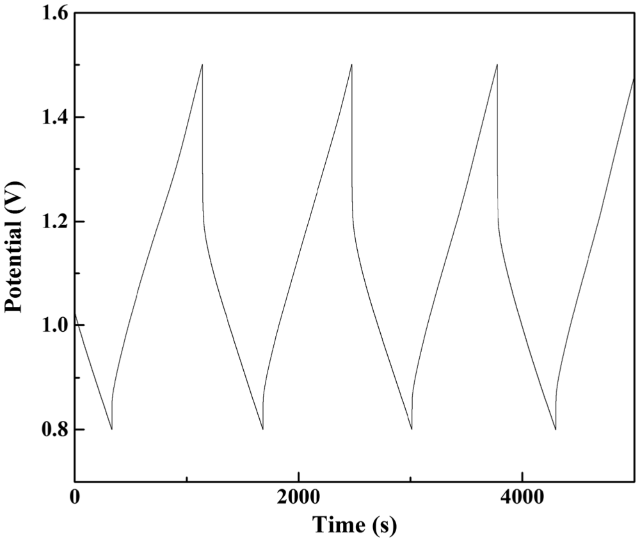

Fig. 8 Variation of discharge capacity of the redox capacitor upon continuous charging and discharging under a constant current of 10 μA

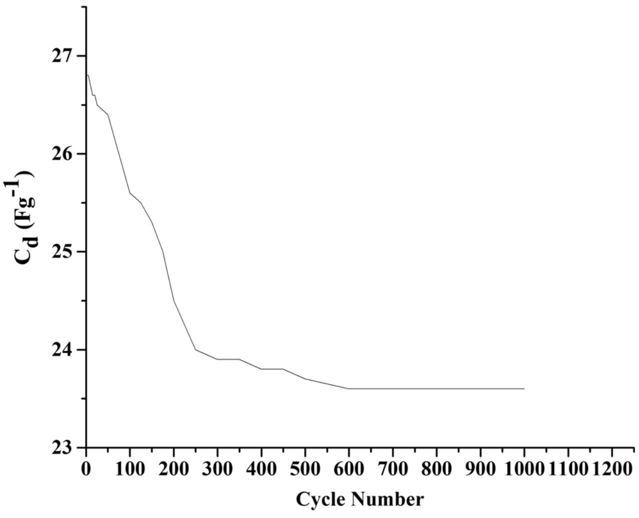

Fig. 9 Variation of discharge capacity of the redox capacitor upon continuous cycling

Galvanostatic charge discharge test

Figure 8 illustrates few charge discharge cycles resulted from the galvanostatic charge discharge test. A sudden decrement of potential could be seen at the onset of discharge. This arises due to ohmic loss across the internal resistance of the device. In general, it is called as *IR* drop. It was slightly higher (0.2 V) in the redox capacitor investigated under the present study. It evidences the high internal resistance.

Figure 9 shows the variation of discharge capacity the redox capacitor upon continuous cycling. However, the important feature that can be observed here is that the capacity degradation over repeated cycling was rather low (~10%). This is an evidence for the stability of PPy film for continuous charging and discharging in a non-aqueous environment. Palaniappan et al. have reported the possible degradation of a conducting polymer (polyaniline) during continuous cycling in an aqueous medium [9].

The calculated average C_d value is 24 F g^{-1}.

Conclusion

A PEO-based nanocomposite polymer electrolyte was successfully prepared using solvent casting method and by optimizing the PEO/$NaClO_4$ molar ratio, PC, and TiO_2 concentrations. The composition used is [{(10PEO: $NaClO_4$) molar ratio}: 75 wt.% PC]: 5 wt.% TiO_2. It showed an ambient temperature ionic conductivity of 5.42×10^{-3} S cm^{-1}. A substantial conductivity enhancement was achieved upon the introduction of PC and TiO_2. Sample was predominantly an ionic conductor. A redox capacitor fabricated with PPy electrodes showed a specific capacity variation between 58 and 83 F g^{-1}. The discharge capacity was 24 F g^{-1}. As a final conclusion, it can be stated that the electrolyte/electrode combination investigated in the study is suitable for using in practical redox capacitors even though the obtained values are quite lower. Further studies are being carried out to improve the performance.

Acknowledgements The authors would like to extend their gratitude to the National Institute of Fundamental Studies, Hantana, Kandy, Sri Lanka, National Science Foundation Sri Lanka (RG/2014/BS/01 and RG/2015/EQ/07), and Wayamba University of Sri Lanka, Kuliyapitiya, Sri Lanka (SRHDC/RP/04/13-01 and SRHDC/RP/04/16-17(R2)).

References

1. Fenton DE, Parker JM, Wright PV (1973) Complexes of alkali metal ions with poly(ethylene oxide). Polymer 14:589
2. Armand M, Chabagno JM, Duclot M (1979) In: Vashista P, Mundy JM, Sheny GK (Ed), Fast ion transport in solids, North Holland, p. 135
3. Kumar KK, Ravi M, Pavani Y, Bhavani S, Sharma AK, Sharma VVRN (2012) Electrical conduction mechanism in NaCl complexed PEO/PVP polymer blend electrolytes. J Non-Crystalline Solids 358(23):3205
4. Agrawal RC, Sahu DK, Mahipal YK, Ashrafi R (2013) Ion transport property of hot press cast Mg^{2+} ion conducting nano composite polymer membranes : study of effect of a ctive/passive filled particle dispersal on conductivity. Indian J Pure Appl Phys 51:320–323
5. Croce F, Settimi L, Scrosati B, Zane D (2006) Nano composite, PEO-LiBOB polymer electrolytes for low temperature, lithium rechargeable batteries. J New Mat Electrochem Syst 9:3–9
6. Jayathilaka PARD, Dissanayake MAKL, Albinsson I, Mellander BE (2002) Effect of nanoporous Al_2O_3 on thermal, dielectric and transport properties of the $(PEO)_9$LiTFSI polymer electrolyte system. Electrochim Acta 47:3257–3268
7. Croce F, Appetecchi GB, Persi L, Scrosati B (1998) Nanocomposite polymer electrolytes for lithium batteries. Nature 394:456–458
8. Nimah YL, Cheng MY, Cheng JH, Rick J, Hwang BJ (2015) Solid state polymer nano composite electrolyte of TiO_2 / PEO / $NaClO_4$ for Na ion batteries. J Power Sources 278:1375–1381
9. Palaniappan S, Sydulu SB, Prasanna TL, Srinivas P (2011) High temperature oxidation of aniline to highly ordered PANI sulfate salt with a nano fiber morphology and its use as electrode material in symmetric super capacitors. J App Polym Sci 120:780–788
10. Chee WK, Lim HN, Huang NM (2015) Electrochemical properties of free-standing polypyrrole/graphene oxide/zinc oxide flexible super capacitor. Int J Energy Res 39:344–355
11. Bandaranayake CM, Jayathilake YMCD, Vidanapathirana KP, Perera KS (2015) Performance of a sodium thiocyanate based gel polymer electrolyte in redox capacitors. J Sabaragamuwa Univ 14(2):149–161
12. Tripathi SK, Jain A, Gupta A, Kumari M (2013) Studies on redox supercapacitor using electrochemically synthesized polypyrrole as electrode material using blend polymer gel electrolyte. Indian J Pure Appl Phys 51:315–319
13. Gupta A, Tripathi SK (2013) Effect of anionic size of PMMA based polymer gel electrolytes for redox capacitors. Int J Eng Res Appl 3(1):1908–1911
14. Tey JP, Careem MA, Yarmo MA, Arof AK (2016) Durian shell based activated carbon electrode for EDLCs. Ionics 21(5):1391–1398
15. Kimura K, Hassoun J, Panero S, Scrosati B, Tominaga Y (2015) Electrochemical properties of a poly(ethylene carbonate)-LiTFSI electrolyte containing a pyrrolidinium-based ionic liquid. Ionics 21(3):895–900
16. Singh PK, Bhattacharya B, Nagarale RK (2010) Effect of Nano TiO_2 dispersion on PEO polymer electrolyte property. J Appl Polym Sci 118:2976–2980
17. Dissanayake MAKL, Jayathilaka PARD, Bokalawela RSP, Albinsonv I, Mellander BE (2003) Effect of concentration and grain size of alumina filler on the ionic conductivity enhancement of the $(PEO)_9LiCF_3SO_3$:Al_2O_3 composite polymer electrolyte. J Power Sources 119-121:409–414
18. Scrosati B, Croce F, Persi L (2000) Impedance spectroscopy study of PEO-based nanocomposite polymer electrolytes. J Electrochem Soc 147:1718–1721
19. Dey A, Karan S, De SK (2013) Effect of nano additives on ionic conductivity of solid polymer electrolytes. Indian J Pure Appl Phys 51:281–288
20. Jayathilake YMCD, Perera KS, Vidanapathirana KP, Bandara LRAK (2014) A novel gel polymer electrolyte based on polymethylmethacrylate and copper trifluoromethanesulfonate. J Electroanal Chem 724:125–129
21. Jyothi NK, Kumar KV, Murthy PN (2014) FTIR, XRD and DC conductivity studies of proton conducting gel polymer electrolytes based on polyacrylonitrile. Int J Chem Tech Res 6(13):5214–5219
22. Bandaranayake CM, Samarakkody GS, Perera KS, Vidanapathirana KP (2016) Variation of performance of dye-sensitized solar cells with the salt concentration of the electrolyte. J Electrochem Energy Conversion Storage 13(1):0110071–0110074
23. Uppugalla S, Male U, Srinivasan P (2014) Design and synthesis of heteroatoms doped carbon/polyaniline hybrid materials for high performance electrode in super capacitor application. Electrochim Acta 146:242–248
24. Bandaranayake CM, Weerasinghe WADSS, Vidanapathirana KP, Perera KS (2015) A cyclic voltammetry study of a gel polymer electrolyte based redox-capacitor. Sri Lankan J Phys 16:19–27
25. Ramya S, Ivasubramanian R, Sangaranarayanan MV (2013) Conducting polymers based electrochemical supercapcitors—progress and prospects. Electrochim Acta 101:109–129
26. Hashmi SA, Lathem RJ, Linford RG, Schlindwein WS (1997) Polymer electrolyte based solid state redox supercapacitor with poly(3 methyl thiophene) and polypyrrole conducting polymer electrodes. Ionics 3:177–183
27. Hashmi SA, Upadhyaya HM (2002) Polypyrrole and poly3 methyl thiophene based solid state redox super capacitors using ion conducting polymer electrolytes. Solid State Ionics 152-153:883–889